

Diagnostic of laser induced Li II plasma

Banaz Omar, August Wierling, Heidi Reinholz, and Gerd Röpke

Institut für Physik, Universität Rostock, Universitätsplatz 3, 18051 Rostock, Germany

Research Article

Received: 30 December 2012

Accepted: XX December 20XX

Online Ready: XX December 20XX

Abstract

Spectral line broadening in dense plasmas is investigated for lithium He-like ion based on a microscopic quantum-statistical approach. By using thermodynamic Greens function, perturber-radiator interaction, plasma correlation and screening effects are taken into account. Ions are treated in quasi-static approximation, leading to a Stark effect by the surrounding perturbers microfield. Stark broadening of Li II ($2p^3P_{2,1,0} - 2s^3S_1$) 548 nm line is calculated, plasma parameters such as temperature and free electron density for the expanding Li plasma after 60 ns from laser irradiation are analyzed (Doria, D., Kavanagh, K.D., Costello, J.T., and Luna, H. (2006) Meas. Sci. Technol., 17, 670-674). The estimated spatial electron density and temperature ranges are $n_e = (0.25-2) \times 10^{24} \text{ m}^{-3}$ and $T \approx (2-3.5) \text{ eV}$, respectively. The dependence of plasma parameters on the line width is investigated. A good agreement is shown by comparing our calculation with the published measured profiles.

Keywords: Stark broadening; Greens function; plasma diagnostic

2010 Mathematics Subject Classification: 53C25; 83C05; 57N16

1 Introduction

Spectral line calculation is an interesting tool for plasma diagnostic. A radiating atom in dense plasmas is perturbed by the influence of surrounding particles, the perturbation leads to the shift and broadening of the line profile, the most dominating effect is Stark broadening. The diagnostic of the spatial and temporal distribution of plasma parameters in a laser-produced plasma is of great interest to many fields in science. Spectral line broadening of Li has industrial applications, lithium is used as a sources for EUV lithography and for soft x-ray emission. The plasma parameters, such as free electron density and temperature can be determined directly from calculated line profile in dense plasmas [Griem (1974)]. The temperature and density distributions are useful for fabrication of thin film materials such as high-temperature superconductors [Bäuerle (1998)].

In this paper we analyze the experimental result of laser-produced Li II plasma at time delay 60 nm, the experiment have been carried out by Doria et al. [Doria et al. (2006)]. Time and spatially

*Corresponding author: E-mail:banaz.omar@uni-rostock.de

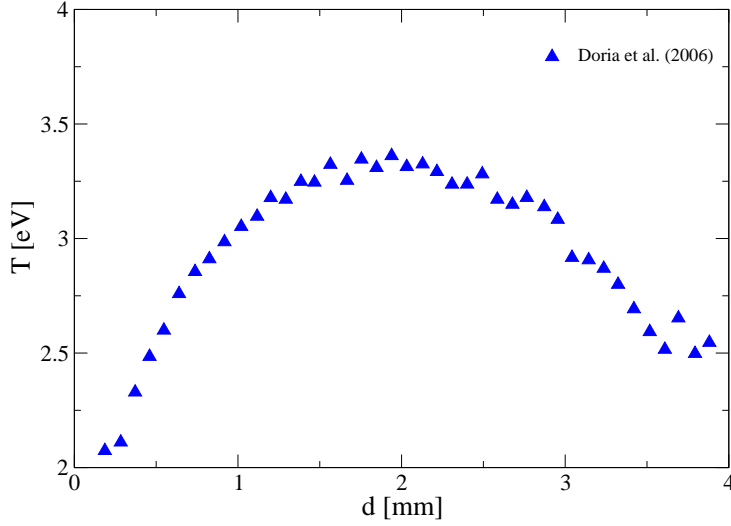


Figure 1: Spatial temperature profile of Li II in one dimension after 60 ns time delay, estimated in Ref. [Doria et al. (2006)].

resolved spectra were measured in one dimension along the plasma expansion normal to a Li target by using a time gated intensified charge-coupled device (ICCD) coupled to a stigmatic spectrometer. A Q-switched Nd:YAG laser $\lambda = 1064$ nm was used with pulse duration 15 ns and 10 Hz repetition rate, the laser was focused onto a pure Li sample surface placed inside a vacuum chamber (5×10^{-5} mbar) generating a plasma that expands normal to the target surface. The laser irradiance was kept constant at an average of 1.3×10^{10} W cm². Laser-induced plasma parameters such as electron temperature, density and plume velocity were extracted directly from the image analysis which has been automated using a MATLAB code. The technique permitted rapid and ready characterization of laser plasma plumes in the early stage of the plasma expansion [Doria et al. (2006)]. The temperature was determined from line intensity ratio of successively charged ions, which is the widely used technique. The spatial profile of the electron density was also estimated by using semiclassical perturbation formalisms from standard theory (ST) of Griem [Griem (1974)]. The ST is a semiclassical approach, where electrons are treated by using impact approximation with a cut-off procedure, while the interaction of ions at radiating particle is given in a quasi-static approximation due to the static microfield distribution function.

The quantum-mechanical Greens function method is considered in this paper to calculate the Li II spectral lines in dense plasmas, assuming local thermal equilibrium (LTE) [Kraeft et al. (1986); Günter and Könies (1994); Sorge et al. (2000); Omar et al. (2006)]. In Sec. 2 an overview of the spectral line modeling is given. Result and discussion are shown in Sec. 3. Comparison with the experimental results of Doria et al. [Doria et al. (2006)] is presented. Finally, conclusion is given in Sec. 4.

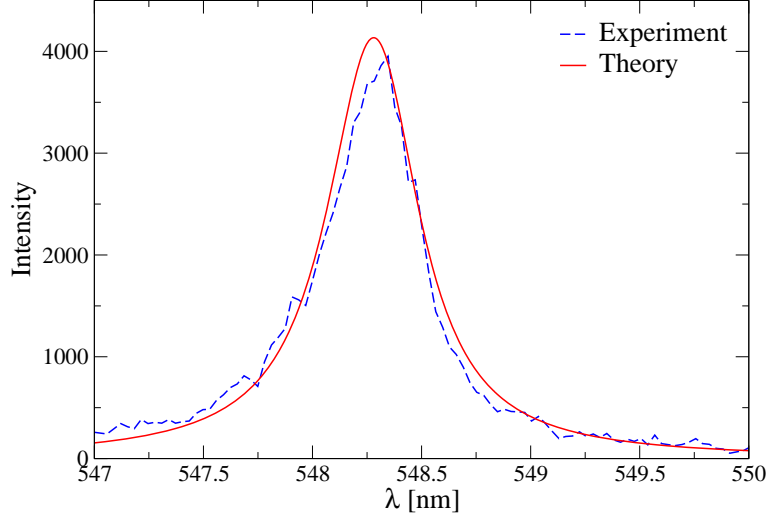


Figure 2: Pressure broadening of the line 548 nm Li II versus wavelength, theoretical profile at $n_e = 1.6 \times 10^{18} \text{ cm}^{-3}$ compared with the measurement [Doria et al. (2006)] at $n_e = 1.885 \times 10^{18} \text{ cm}^{-3}$, $T = 2.46 \text{ eV}$, and $d = 0.43 \text{ mm}$.

2 Theoretical approach of pressure broadening in dense plasmas

Spectral line shape is given by the second order two-particle polarization function, which is a bound-bound transition. The polarization function is calculated in a systematic way from thermodynamic Greens function, which is proportional to the Fourier transform of the dipole-dipole autocorrelation function. The perturber-radiator interaction leads to a pressure broadening, which contains an electronic and an ionic contributions. Including the ionic contribution in the quasi-static approximation by averaging over the ionic microfield [Sorge et al. (2000)], we have

$$I^{\text{pr}}(\omega) \sim \sum_{i', i'', f', f''} \langle i' | \mathbf{r} | f' \rangle \langle f'' | \mathbf{r} | i'' \rangle \frac{\omega^4}{8\pi^3 c^3} e^{-\frac{\hbar\omega}{k_B T}} \int_0^\infty W(\beta) d\beta \times \text{Im} \langle i' | \langle f' | [\hbar\omega - \hbar\omega_{if} - \Sigma_{if}(\omega, \beta) + i\Gamma_{if}^v]^{-1} | f'' \rangle | i'' \rangle, \quad (2.1)$$

where $\langle i | \mathbf{r} | f \rangle$ is identified as a dipole matrix-element for the transition between initial $n_i l_i m_i$ and final $n_f l_f m_f$ states. The vertex correction Γ_{if}^v for the overlapping line is related to coupling between the initial and the final states [Kraeft et al. (1986)]. The ionic microfield distribution function $W(\beta)$ is taken according to Ref. [Hooper (1968)] with field strength $\beta = E/E_0$ normalized to the Holtsmark field E_0 , and $\hbar\omega_{if} = E_i - E_f$ is the unperturbed transition energy. The function $\Sigma_{if}(\omega, \beta)$ is determined by the self-energy correction $\Sigma_n(\omega, \beta)$ of the initial and the final states

$$\Sigma_{if}(\omega, \beta) = \text{Re}[\Sigma_i(\omega, \beta) - \Sigma_f(\omega, \beta)] + i \text{Im}[\Sigma_i(\omega, \beta) + \Sigma_f(\omega, \beta)], \quad (2.2)$$

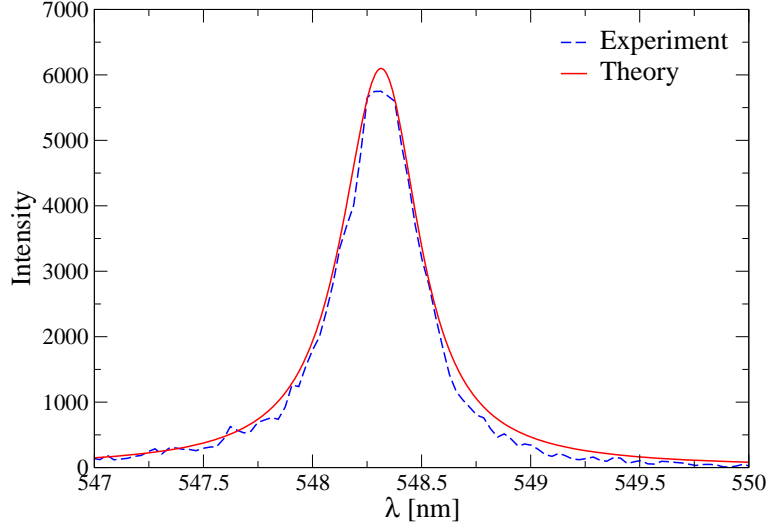


Figure 3: The calculated line shape of Li II 548 nm vs. λ at $n_e = 1.35 \times 10^{18} \text{ cm}^{-3}$ and $T = 2.69 \text{ eV}$. Comparison is made with the measured profile in Ref. [Doria et al. (2006)] at $n_e = 1.402 \times 10^{18} \text{ cm}^{-3}$ for the same temperature at distance $d = 0.6 \text{ mm}$.

where the real part represents the shift and the imaginary part gives the width of each state. The electronic and ionic contributions occur in the self-energy

$$\Sigma_n(\omega, \beta) = \Sigma_n^{\text{ion}}(\beta) + \Sigma_n^{\text{el}}(\omega, \beta) . \quad (2.3)$$

Performing Born approximation with respect to the dynamically screened perturber-radiator potential, the electronic self-energy is obtained as

$$\begin{aligned} \Delta_n^{\text{SE}} + i\Gamma_n^{\text{SE}} &= \langle n | \Sigma^{\text{el}}(E_n, \beta) | n \rangle = -\frac{1}{e^2} \int \frac{d^3q}{(2\pi)^3} V(q) \sum_{\alpha} |M_{n\alpha}(\mathbf{q})|^2 \\ &\times \int_{-\infty}^{\infty} \frac{d\omega}{\pi} [1 + n_B(\omega)] \frac{\text{Im} \varepsilon^{-1}(\mathbf{q}, \omega + i0)}{E_n - E_{\alpha}(\beta) - \hbar(\omega + i0)} . \end{aligned} \quad (2.4)$$

Here, the level splitting ($E_{\alpha}(\beta) \approx E_{\alpha}$) due to the microfield has been neglected [Günter and Könies (1994)], $n_B(\omega) = [\exp(\hbar\omega/k_B T) - 1]^{-1}$ is the Bose distribution function, and the sum over α runs from $n - 2$ to $n + 2$ discrete bound states for the virtual transitions. Dynamical screening effect is accounted for in Eq. (2.4) from imaginary part of the inverse dielectric function $\varepsilon^{-1}(\mathbf{q}, \omega)$, which is approximated by random phase approximation (RPA). The transition matrix-element $M_{n\alpha}(\mathbf{q})$ describes the interaction of the atom with the Coulomb potential through the vertex function. The Coulomb interaction with electron-electron-ion triplet depends on the momentum transfer $\hbar\mathbf{q}$ [Kraeft et al. (1986)]. The matrix-element of He and He-like ions can be approximated by the one of hydrogen, while the outer electron is screened by inner electron [Omar et al. (2006)]. The electronic wavefunction for singly ionized Li is obtained by applying Coulomb approximation method [Bates and

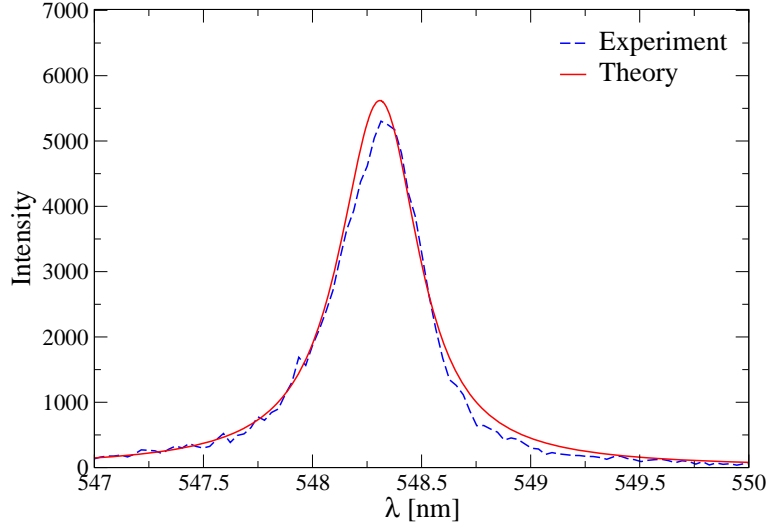


Figure 4: The calculated line profile of Li II 548 nm versus wavelength at $n_e = 1.376 \times 10^{18} \text{ cm}^{-3}$ and $T = 2.58 \text{ eV}$. Comparison is made with the measured line [Doria et al. (2006)] at estimated electron density $n_e = 1.38 \times 10^{18} \text{ cm}^{-3}$ and distance $d = 0.53 \text{ mm}$.

Damgaard (1949)]. In this approximation the wavefunction and radial part of the transition matrix-element are expressed in terms of $[P_{nl}(r) = r \psi_{nl}(r)]$ and σ , respectively. To verify the wavefunction, the absorption oscillator strength of transition f_{if} and σ^2 of the singly excited states of Li II are indicated as [Wiese and Fuhr (2009); Bethe (1977); Cohen and Kelly (1967); Theodosiou (1985)]

$$f(1snlSLJ - 1sn'l'S'L'J') = \frac{1}{3} \frac{\Delta E}{R} \frac{2S+1}{2J'+1} \delta(SS') \max(l, l') \left(\int_0^\infty r P_{nl}(r) P_{n'l'}(r) dr \right)^2, \quad (2.5)$$

where R is the reduced mass Rydberg constant, and ΔE is the transition energy.

Considering Born approximation, the electronic part is overestimated, to avoid this we apply the cut-off procedure and add a strong collision term [Griem (1974, 1988); Griem et al (1990)] in stated of partial summation of the three-particle T-matrix, where the result might be slightly modified. For Li II we adopt the cut-off parameter $\rho_{\min} = n^2/Z$, where Z is the effective charge [Griem (1988)]. The close electron-radiator collision term is evaluated according to the semiclassical estimation in Refs. [Griem (1988); Griem et al (1990); Griem et al. (1979); Nguyen et al. (1986)]

$$\phi_{\text{SC}} = -\frac{4\pi}{3} \left(\frac{2m_e}{\pi k_B T} \right)^{1/2} n_e \left(\frac{\hbar}{m_e} \right)^2 |< nl|r|nl >|^2 C_{nl}, \quad (2.6)$$

where C_{nl} is the strong collision constant and $< nl|r|nl >$ is the dipole matrix-element.

For non-hydrogenic radiator, ionic contribution to the self-energy is related to quadratic Stark effect and quadrupole interaction, further detail is given in Refs. [Sorge et al. (2000); Omar et al. (2006)]. The microfield can be considered as a static microfield distribution function, while it does not change during the time of interest for the radiation process.

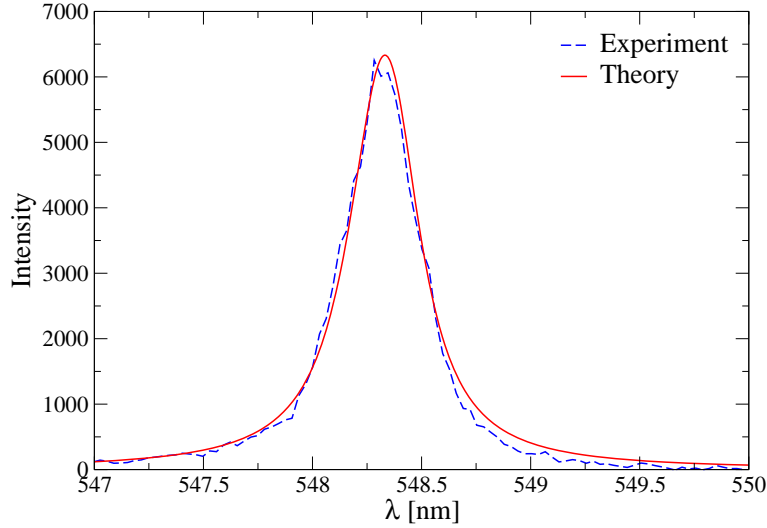


Figure 5: Stark broadening of the Li II line 548 nm versus wavelength. The calculated profile at $n_e = 1.2 \times 10^{18} \text{ cm}^{-3}$ compared with the measured one at $n_e = 0.982 \times 10^{18} \text{ cm}^{-3}$, $T = 2.77 \text{ eV}$ and $d = 0.676 \text{ mm}$ [Doria et al. (2006)].

3 Result and Discussion

In this section, we perform the pressure line broadening and the related full width at half maximum (FWHM) of the Li II 548 nm line by applying the approach outlined above. The comparison between our theoretical calculation and experimental results is shown, assuming LTE. The time-resolved measured profiles are space resolved along the direction of expansion, the observed plasma parameters such as relative line intensities and Stark broadening parameters have been extracted from the profiles [Doria et al. (2006)]. Under the assumption of LTE, the spatial electron temperature profile was evaluated from the intensity ratio of Li II at two isolated lines 548 nm and 467 nm, see Fig. 1 [Doria et al. (2006); Griem (1964)]. The relative intensities were corrected according to the wavelength dependence of the spectral sensitivity of the spectrometer. The statistical error in the intensity ratio was less than 3% for distances between 1 mm to 3 mm from the sample surface, but increased up to 10% further away at the edges of the plasma plume, where distance $d = 0$ at the target surface.

Stark broadening parameters are calculated from Eq. 2.4 by using thermodynamic Greens function, the cut-off procedure is adopted and the strong collision term is added by using Eq. 2.6 according to Griem and his collaborators [Griem (1988); Griem et al (1990)]. The ionic contribution is taken into account from second-order perturbation theory which is known as the quadratic Stark effect [Bethe (1977)]. Ions are treated in quasi-static approximation by using microfield distribution function of Hooper [Hooper (1968)], the comparison is done with the distribution function given in Ref. [Sadykova et al. (2009)], where no sensible difference has been observed. The pressure line broadening is evaluated from Eq. 2.1 and compared with the measurement [Doria et al. (2006)], given in Figs. 2-7. Then the electron density and the FWHM are estimated from the best-fitting profile with the measurement, illustrated in Figs. 8 and 9, respectively. The plasma expands freely and cooling

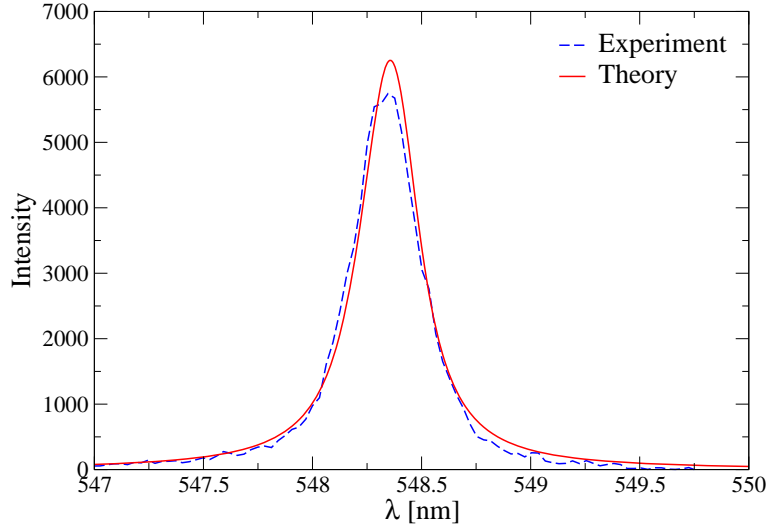


Figure 6: Comparison of the theoretical and measured line shapes of the Li II 548 nm line vs. wavelength at $n_e = 1.0 \times 10^{18} \text{ cm}^{-3}$ and $n_e = 0.962 \times 10^{18} \text{ cm}^{-3}$, respectively, at $T = 2.96 \text{ eV}$ and $d = 0.89 \text{ mm}$ [Doria et al. (2006)].

down while the electron density decreases with increasing d normal to the surface. The gradient of density as a function of d in one dimension after 60 ns of laser exposure is shown in Fig. 8. The electron density profile was indicated in Ref. [Doria et al. (2006)] from line broadening by extrapolating the tabled values of Griem [Griem (1974)]. The highest value of the electron density observed near the target surface, by plasma cooling n_e decreases rapidly with increasing d due to condensation and recombination. In Fig. 8 the variation of n_e near the surface is in a good agreement with the estimation in Ref. [Doria et al. (2006)], while the discrepancy can be seen with increasing d . The first region is a transient region, rapid change in electron density can be seen and the second part is related to the plasma equilibrium, where n_e is almost constant. The Doppler broadening becomes less important with increasing density, and the width is only due to Stark broadening at high density. Regarding the data reported in Ref. [Doria et al. (2006)], the discrepancy may be due to the self-absorption.

The accuracy of calculating electronic dipole matrix-elements is approved by comparing our results of f_{if} and σ with the other calculated values in Ref. [Theodosiou (1985); Cohen and Kelly (1967); Ateş and Çelik (2009)], see table 1, very good agreement can be seen.

4 Conclusions

In this study, diagnostic of laser induced lithium plasma by Doria et al. [Doria et al. (2006)] is performed. The quantum statistical approach is presented to the line profile calculation of allowed isolated Li II 548 nm, this method is applicable for both allowed and forbidden radiative transitions. A cut off procedure is used for strong collisions according to Griem [Griem (1974)]. The Coulomb approximation is employed to evaluate the wavefunctions of Li II. In our calculation, the time-dependent

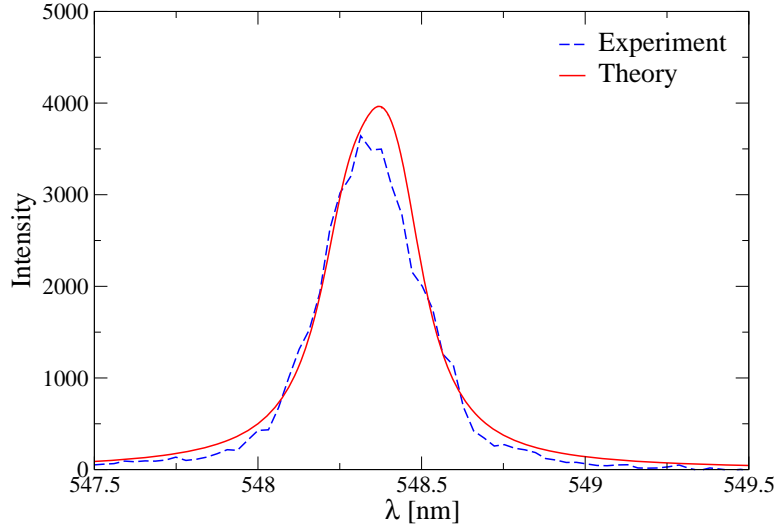


Figure 7: The line profiles of Li II 548 nm line versus wavelength. Our calculation at $n_e = 0.8 \times 10^{18} \text{ cm}^{-3}$ compared with the profile measured in Ref. [Doria et al. (2006)] at $n_e = 0.561 \times 10^{18} \text{ cm}^{-3}$, $T = 3.31 \text{ eV}$, and $d = 1.53 \text{ mm}$.

microfield fluctuation is approximated by its static value due to the large mass of the ion relative to the electron mass, assuming the stationary motion of ions during the time of collisions. The contribution of ions is taken into account within quadratic Stark effect in the quasi-static approximation. The spatial distribution of the electron density is estimated along the direction of plasma plume expansion. Good agreement can be clearly seen by comparing our line profiles with the measured profiles. However, the estimated values of n_e in Ref. Doria et al. (2006) are overestimated systematically with increasing distance.

References

- Griem, H.R. (1974). *Spectral Line Broadening by Plasmas*: Academic Press, New York.
- Bäuerle, D. (1998). *Pulsed-laser deposition and characterization of high-temperature superconductors*. Supercond. Sci. Technol., 11, 968-972.
- Doria, D., Kavanagh, K.D., Costello, J.T., and Luna H. (2006). *Plasma parametrization by analysis of time-resolved laser plasma image spectra*. Meas. Sci. Technol., 17, 670-674.
- Kraeft, W-D., Kremp, D., Ebeling, W., and Röpke, G. (1986). *Quantum Statistics of Charged Particle Systems*: Akademie-Verlag, Berlin.
- Günter, S. and Könies, A. (1994). *Quantum mechanical electronic width and shift of spectral lines over the full line profile-electronic asymmetry*. Quant. Spectrosc. Radiat. Transfer, 52, 819-824.

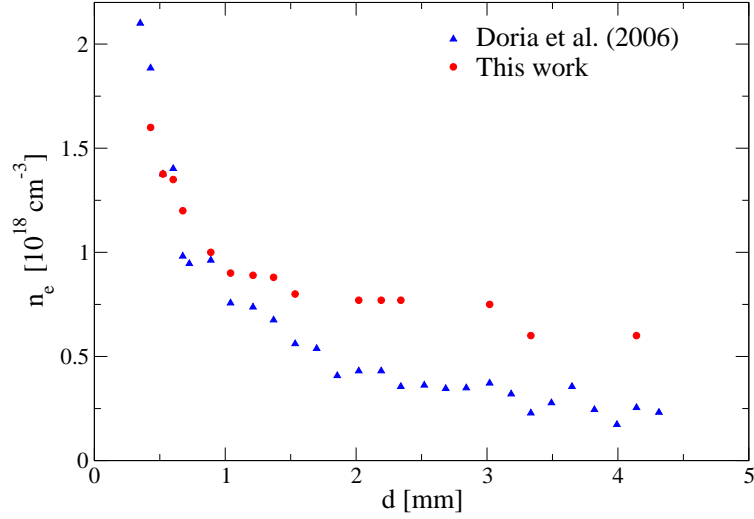


Figure 8: The free electron density distribution of Li II versus normal distance from the sample surface d . Comparison is made with the estimation values in Ref. [Doria et al. (2006)] at 60 ns delay time.

Sorge, S., Wierling, A., Röpke, G., Theobald, W., Sauerbrey, R., and Wilhein, T. (2000). *Diagnostics of a laser-induced dense plasma by hydrogen-like carbon spectra*. J. Phys. B: At. Mol. Opt. Phys., 33, 2983-3000.

Omar, B., Günter, S., Wierling, A., and Röpke, G. (2006). *Neutral helium spectral lines in dense plasmas*. Phys. Rev. E, 73, 056405-13.

Hooper, C. F. Jr (1968). *Low-frequency component electric microfield distribution in plasmas*. Phys. Rev., 165, 215-222.

Bates, D.R. and Damgaard, A. (1949). *The calculation of the absolute strengths of spectral lines*. Phil. Trans. Roy. Soc. London, A 242, 101-122.

Wiese, W. L. and Fuhr, J. R. (2009). *Accurate Atomic Transition Probabilities for Hydrogen, Helium, and Lithium*: published online 24 June 2009; publisher error corrected 23 September

Bethe, H.A. and Salpeter, E.E. (1977). *Quantum Mechanics of One- and Two- Electron Atoms*: Plenum Publishing Corporation, New York.

Cohen, M. and Kelly, P.S. (1967). *Hartree-Fock wave function for excited states. IV. oscillator strength in the helium isoelectronic sequence*. Can. J. Phys., 45, 2079-.

Theodosiou, C.E. (1985). *Lifetimes of the Singly Excited States in Li I I*. Physica Scripta, 32, 129-133.

Griem, H.R. (1988). *Shifts of hydrogen and ionized-helium lines from $\Delta n = 0$ interactions with electrons in dense plasmas*. Phys. Rev. A, 38, 2943-2952.

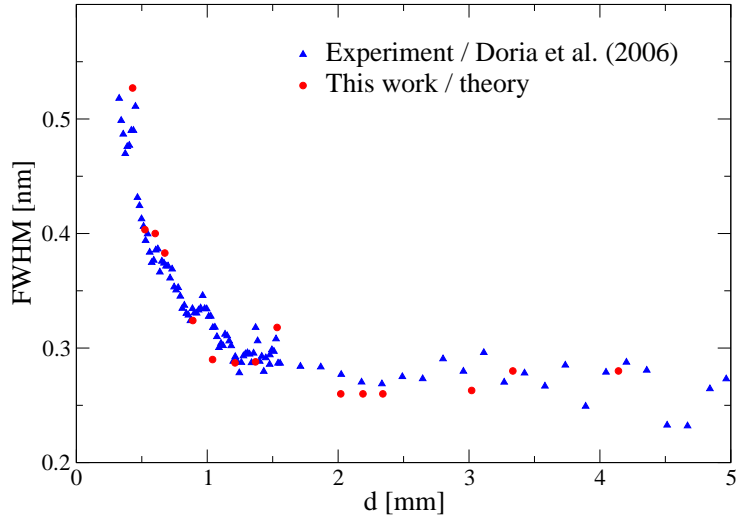


Figure 9: The FWHM of Li II ($2p^3P_{2,1,0} - 2s^3S_1$) 548 nm line versus distance. Comparison is made with the estimated values from measured profiles after 60 ns laser exposure [Doria et al. (2006)].

Griem, H.R., Blaha, M., Kepple, P.C. (1990). *Stark-profile calculations for resonance lines of heliumlike argon in dense plasmas*. Phys. Rev. A, 10, 5600-5609.

Griem, H.R., Blaha, M., Kepple, P.C. (1979). *Stark-profile calculations for Lyman-series lines of one-electron ions in dense plasmas*. Phys. Rev. A, 19, 2421-2432.

Nguyen, H., Koenig, M., Benredjem, D., Caby, M., and Coulaud, G. (1986). *Atomic structure and polarization line shift in dense and hot plasmas*. Phys. Rev. A, 33, 1279-1290.

Griem, H.R. (1964). *Plasma Spectroscopy*. McGraw-Hill, New York.

Sadykova, S., Ebeling, W., Valuev, I., and Sokolov, I. (2009) *Electric microfield distributions in Li^+ plasma with account of the ion structure*. Contr. Plasma Phys., 49, 76-89.

Ateş, Ş. and Çelik, G. (2009) *Oscillator Strengths for Allowed Transitions in Li II*. Acta Physica Polonica A, 116, 169-175

Transition	σ^2	σ^2 ⁽¹⁾	f_{if}	f_{if} ⁽¹⁾	f_{if} ⁽²⁾
³ S- ³ P ⁰ 2s-2p	1.85014	1.894	0.307485	0.323	0.30665/0.307940
-3p	0.240332	0.2361	0.182895	0.179	0.18330/0.1871
-4p	0.0627511	0.0578	0.0605617	-	0.05637/0.0575
3s-2p	0.210062	0.2201	0.115857	-	0.11416/0.11710
-3p	11.8357	11.93	0.512237	-	0.51167/0.5128
-4p	0.7274	0.7274	0.179942	-	0.18583/0.18686
4s-2p	0.0270884	0.0280	0.0211708	-	0.020787/0.02147
-3p	1.36309	1.413	0.254529	-	0.25376/0.2550
-4p	40.69	40.69	0.706735	-	0.70298/0.7036

Table 1: Comparison is given between our calculated values of σ^2 and f_{if} for triplet transition of Li II and those in Refs. ⁽¹⁾[Cohen and Kelly (1967)] and ⁽²⁾[Theodosiou (1985)].